

Through-focus or volumetric type of optical imaging methods: a review

Ravi Kiran Attota*

Engineering Physics Division, PML, National Institute of Standards and Technology
Gaithersburg, MD 20899, USA

*Ravikiran.attota@nist.gov

Abstract. In recent years the use of through-focus (TF) or volumetric type of optical imaging has gained momentum in several areas such as biological imaging, microscopy, adaptive optics, material processing, optical data storage, and optical inspection. In this paper, we provide a review of basic TF optical methods highlighting their design, major unique characteristics, and application space.

Keywords: Through-focus imaging, optical microscope, optical imaging, TSOM, volumetric imaging, out-of-focus imaging, extended-depth-of-field imaging, axial scanning, three-dimensional imaging, bioimaging

1 Introduction

Considerable progress has been made in the area of optical microscopes and their applications during the past two decades (1-8). Optical tools with numerous variations and techniques have become a major part of research and development in the bio-related fields. Usage of through-focus (TF) optical imaging is steadily gaining momentum, particularly in biological applications (9-16). TF imaging is sometimes informally and interchangeably referred to using terms such as volumetric, out-of-focus, blurred, defocused, extended-focused, extended-depth-of-field, axial scanning, and three-dimensional (3D) imaging.

Several uses of the TF optical image applications such as biological imaging, microscopy, adaptive optics, material processing, optical data storage, and optical inspection have been reported (17). In this paragraph we highlight some specific applications and methods that use TF images. TF scanning optical microscopy (TSOM) makes use of a set of defocus optical images for three-dimensional shape metrology of target sizes ranging from sub-10 nm to as over 100 nm, including nanoparticles (18, 19), with sub-nanometer resolution(18-37). The ability to analyze optical illumination was also reported (20) using the TSOM method. Much interest is given to two-photon (or multi-photon) microscopy that makes use of TF imaging to acquire 3D volumetric data of biological samples, including brain tissue and bone calcium (11, 14, 15). High speed TF imaging is used to track single-molecules in three dimensions and observe their behavior during cell division (38), and it has also been

used to image entire embryos (39). By simultaneously imaging different focal planes within the sample it was possible to track the 3D dynamics in live cells at high temporal and spatial resolution (12, 13). 3D position, alignment and orientation of submicroscopic features was made possible by TF polarization imaging in label-free as well as fluorescently labeled specimens (40). Cellular network dynamics such as spatiotemporal activity patterns in neuronal and astrocytic networks was demonstrated using TF imaging in 3D (14). 3D automated nanoparticle tracking was demonstrated using TF images (41).

2 Significance of TF image collection

Three important developments have increased the prevalence of TF imaging:

I. TF data conventionally includes out-of-focus or blurred images. These blurred images were once considered to be of either inferior quality or not useful, and were therefore mostly discarded - as in confocal microscopy (42). However, with the development of technology, improved optical simulations and new insights it was found that the out-of-focus TF images do contain useful information regarding the target being imaged. New applications and uses are being found for blurred optical images that were previously considered unusable (20, 29, 32, 34, 43-48). The major challenge was to extract high quality, usable information from the blurred TF optical images. TSOM (18-37) is an example of a method where useful three-dimensional shape information can be extracted from a set of TF, blurred,

optical images. TSOM enables 3D shape metrology with sub-nanometer measurement resolution using a conventional optical microscope (24, 25). TSOM has demonstrated the capability of extracting three-dimensional shape information of targets ranging in size from sub-10 nm to greater than 100 μm , with measurement resolution comparable with scanning electron microscopy (SEM) or atomic force microscopy (AFM).

II. The second development is the advent of new applications that require collection of TF or volumetric data. Examples include high-speed 3D tracking of nanoparticles (38, 41), observation of high-speed cell division (38) and cellular network dynamics in three dimensions (14), and 3D volumetric data of biological samples such as brain tissue and bone calcium (11, 14, 15).

III. The third development is that advances in technology, instrumentation, simulations and computation have enabled collection of TF images with sufficiently high-quality and at sufficiently high-speed to allow TF information to be readily utilized for many applications. For example, the development of objective lens scanning using piezo scanners has made it possible to readily adopt any conventional optical microscope into a high-speed TF image collection tool with acquisition times as small as 200 ms (41). Optical tool developments have also enabled the simultaneous collection of TF images, with no scanning parts (38-40).

It is now firmly established that TF optical images are beneficial for many applications. A survey of prior work reveals that many optical methods for TF image collection have been developed. It would be impossible to describe or even mention all of them in this review. However, most of the methods that have been published are variations of a few unique or basic methods. We here review the TF methods that represent the foundation of most published techniques.

3 Through-focus image collection methods

In this section, we describe most of the basic TF methods that have been published. These methods are depicted using simplified schematics and brief summaries. Note that in the following figures, the portions of the diagrams enclosed using dashed boxes indicate components or aspects of the technique that are unique to that particular method. Note also that some figures (e.g., Fig. 1) depict multiple interrelated techniques.

3.1 Scanning the sample stage along the focus axis

Sample stage scanning, shown schematically in Fig. 1(a), is the classic and the most widely used method to obtain TF images. It is simple and straightforward and nearly every

optical microscope has some provision to adjust the sample along the focus axis: these methods range from manual focusing on basic instruments to more sophisticated motorized or piezo scans on high-end modern tools. The scanning range can be up to several tens of millimeters, and positional accuracy can be better than 10 nm. However, TF scan speeds are typically regarded as relatively slow. Depending on the focus scan range, the exposure time, and the number of focal steps required, the total scan time could extend up to several minutes. The focus accuracy of this TF technique can be among the best, with high reproducibility and low distortion. However, optical mechanical instability (32) and illumination aberrations (49, 50) have also been reported for such systems.

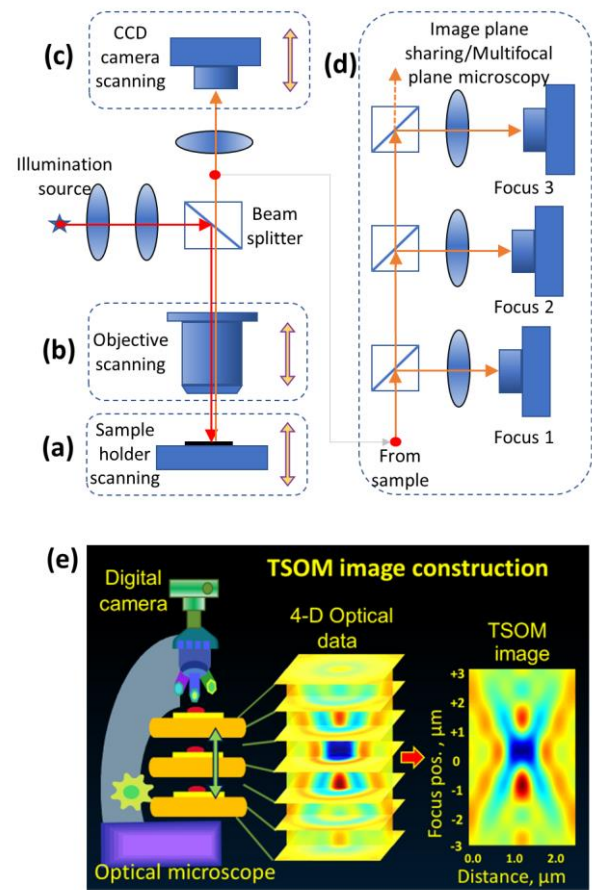


Fig. 1 TF image acquisition methods schematically shown using reflection (epi-illumination) optical microscopes. The methods include axial scanning of (a) the sample holder, (b) the objective lens, or (c) the camera; (d) splitting the imaging beam and focusing it onto multiple cameras set to different focal positions. (e) A typical through-focus scanning optical microscopy image construction using stage-scanning method (Video 1, MPEG, 0.5 MB).

TF optical images collected by the stage-scanning method can be stacked at their respective focus positions to create a 3-D space filled with the optical intensities. Plotting the optical intensities in a vertical cross-section through this 3-D space results in a TSOM image (Fig. 1(e)). Even though TSOM uses conventional optical images (i.e., not a resolution enhancement method), it provides sub-nanometer 3-D shape measurement resolution (24) as it uses additional information present in the out-of-focus optical images. TSOM images are sensitive to changes in the (i) 3-D shape of a target (24, 29), (ii) position of a target in a 3-D space (41), (iii) optical properties of a target, and (iv) illumination (20). A differential TSOM image (pixel-by-pixel difference between two well-aligned TSOM images) highlights all these differences with much higher signal-to-noise ratio compared to a conventional best-focus, top-down optical image (18, 19). TSOM is a strong candidate to analyze the position, shape and optical properties of soft nanoparticles (for example, hydrogel nanoparticles) in their native liquid environment, in addition to hard nanoparticles (41).

3.2 Scanning the objective lens along the focus axis

Another method of collecting TF images is by scanning the objective lens along the focal axis (Fig. 1(b)), generally using piezo motors (14, 41, 51). A relatively high-speed TF image collection time of 200 ms has been reported (41) using this method, which makes it suitable, e.g., for nanoparticle tracking in 3D space. It is relatively easy to convert a conventional microscope into a TF image collecting tool by replacing its objective lens base with one of the several commercially available objective-scanning piezo motors. In this high-speed scanning mode, the image quality could be degraded. However, this approach has the advantage of not disturbing the specimen because the sample stage remains stationary during imaging. Mechanically this method is more stable than the stage scanning method.

3.3 Scanning the image plane along the focus axis

Through focus image collection can also be accomplished by scanning the image plane or camera (12, 32), as shown in Fig. 1(c). The same effect can also be achieved by scanning a replica of the image plane (52). This method is reported to have the advantage of avoiding the spherical aberration common to other optical refocusing systems; it also allows for fast TF scans, extending the working distance, and keeping the specimen on stage stationary and undisturbed (52).

3.4 Multifocal plane microscopy

Instead of scanning the image plane, one alternative is to split the imaging beam into several fixed beams that are refocused simultaneously onto multiple cameras positioned

at different focal distances (12, 13, 32), as shown in Fig. 1(d). This is also called image plane sharing microscopy (32). It has the main advantage of avoiding scanning altogether (of stage, objective or imaging plane). In this configuration, the TF images are collected simultaneously which enables high-speed TF image collection. However, since the imaging beam is split into several beams, the available optical intensity at each camera is reduced - which may lower the signal-to-noise ratio of the optical data, unless the collection time is increased. The number of focal planes available is also limited to the number of times the imaging beam is split. Since there are no moving (scanning) parts, this is one of the most mechanically stable configurations.

3.5 Wavelength scanning method

For microscope objectives with chromatic aberration, differing wavelengths will have different focus positions. Normally microscope objectives are designed to minimize chromatic aberration. However, chromatic aberration can also be used to obtain TF images (32, 34, 53). In this method, both the chromatically aberrated objective and the sample stage are kept at fixed positions. Instead, the wavelength of illumination is varied (or wavelength-scanned) so that each wavelength focuses at a different focus position on the sample, enabling TF image collection (Fig. 2). A variation of this approach, which utilizes the chromatic dependence of diffraction, has been developed using tri-colored LED illumination and a spatial light modulator (SLM) (53). Since the position of sample stage is not scanned, the wavelength scanning approach generally has superior mechanical stability compared to conventional stage-scanning optical microscopes. It also allows high-throughput TF image collection due to the ability to quickly and precisely tune the wavelength (34) (faster than scanning a stage).

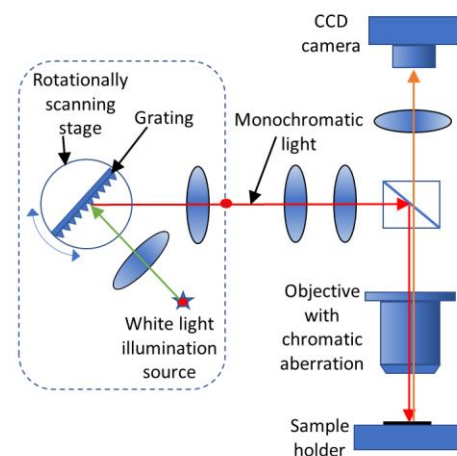


Fig. 2 TF image collection configuration by wavelength-scanning using an objective with chromatic aberration. In the

setup shown here, the white light is split into different wavelengths using a rotationally-scanned grating.

3.6 Flexible-membrane liquid lens

While there are many variations in design and implementation, the general concept of the approach shown in Fig. 3(a) is that the fluid pressure inside two flexible membranes is varied to make the membranes inflate or deflate. This process alters the radius of curvature of the membranes and thus changes the effective focal length of the lens, allowing TF image collection (54-62). The membrane curvature can alternatively be varied by different mechanisms such as changing the aperture diameter thus squeezing the membranes (63). These lenses are generally fast, but are prone to have optical aberrations (56).

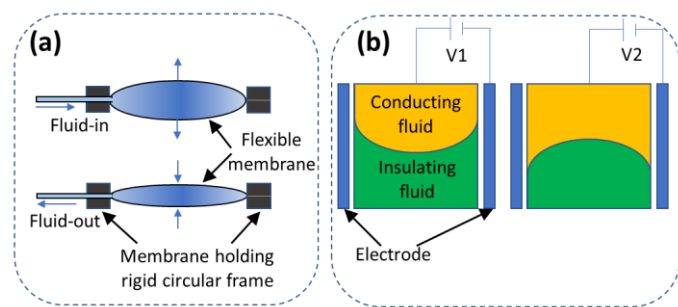


Fig. 3 Focus-Tunable Lenses. (a) Flexible membrane liquid lens. The effective focal length changes due to changes in the curvature of the flexible membranes when the pressure inside is varied. (b) Liquid-tunable lens. The curvature at the interface of two immiscible liquids varies due to changes in the interfacial tension when the applied voltage across the insulating and conducting fluids is changed. The change in the curvature results in varying the focal length.

3.7 Liquid-tunable lens

This method, illustrated in Fig. 3(b), is also known as a variable focus liquid lens. These lenses utilize refraction at a liquid-liquid boundary interface. Focal adjustment is achieved by using a variable voltage to tune the curvature at the boundary interface of two immiscible liquids. A spherical surface is formed at the boundary of a polar and an apolar liquid. The curvature of the interface can be controlled by adjusting the relative wettability through electro-wetting [15]. This creates a lens with variable focal length to enable TF image collection (15, 55, 63, 64). Liquid lenses are relatively fast and very durable and exhibit a high degree of phase shift, i.e., focal length change. These lenses have a long functional life and low sensitivity to mechanical stress, and they are also advantageous for autofocus applications due to their relatively low power consumption. Liquid-

tunable lenses have relatively low cost and are commercially available. However, the optical performance of liquid-tunable lenses suffers from significant spherical as well as higher-order, gravity-induced aberrations (56).

3.8 Adaptive optics

As illustrated in Fig. 4, adaptive optical elements such as a tip/tilt or deformable mirror can be inserted into the optical path of a microscope to enable TF image collection (32, 65, 66). Common examples of adaptive optics elements are deformable mirror devices or liquid crystal spatial light modulators (SLMs). The adaptive optics is used to alter the phase of incident wave fronts to displace the focal spot. Tip/tilt applied to the adaptive optics shifts the focus laterally within the focal plane, while defocus translates along the optic axis (65). In the implementation with a tip/tilt mirror a basic closed-loop quad cell is used to control the mirror. A high-order deformable mirror with a Shack-Hartmann sensor is used in the deformable mirror implementation. This approach can also correct high-order residual aberrations as well as performing the TF scanning without z-axis movement. A key advantage of these methods is high-speed TF image collection (~KHz). Adaptive optics technology and hardware are readily available and are most commonly used for biological applications (16).

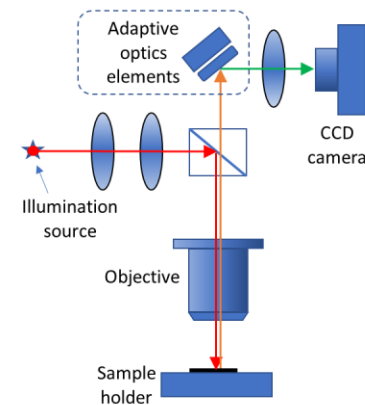


Fig. 4 Schematic showing a design of using adaptive optical elements for TF image collection using tip/tilt or deformable mirrors.

3.9 Multi-focus microscopy (MFM)

MFM allows rapid and simultaneous acquisition of TF images using a single exposure (Fig. 5). Unlike a conventional microscope, there are no scanning parts (38-40). This is achieved by placing a multi-focus grating (MFG) at the Fourier plane followed by a chromatic correction grating (CCG) and prism (Fig. 5(a)). The combination of these elements divides the primary image into several TF images and simultaneously

projects them onto the plane of the CCD camera. Unlike a conventional microscope, the CCD camera in MFM is divided into several squares, each one of which is used to collect one of the focal plane images (Fig. 5(b)). To date, MFM has been used primarily for biology applications, and this technology is not yet widely available.

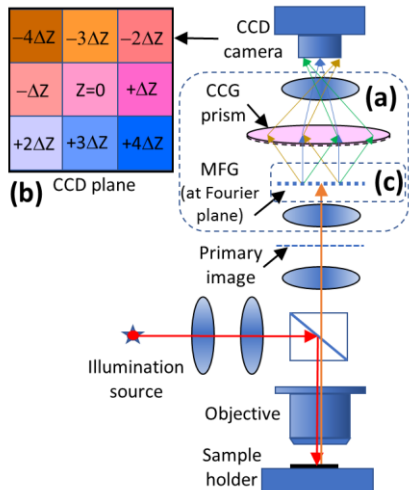


Fig. 5 Simplified schematic of MFM. (a) Optical elements unique to MFM. MFG = multi-focus grating located at the Fourier plane, CCG = chromatic correction grating. (b) Images at predetermined focal planes are collected simultaneously by dividing the camera area as shown here. Optical designs are available to collect 3x3, 4x4 or 5x5 images in the camera. (c) The location of aperture for aperture-scanning Fourier ptychography method.

3.10 Aperture-scanning Fourier ptychography

In this method, an aperture is placed at the Fourier plane as illustrated in Fig. 5(c), and it is scanned in a raster manner while simultaneously collecting intensity images of the object. The acquired images are then synthesized in the frequency domain to recover the complex hologram of extended objects. This can then be digitally propagated into different planes along the optical axis to extract TF images of the object (67). An alternative method is to scan the camera instead of an aperture (67). Because of the requirement to scan certain parts, this approach could be slower.

3.11 Confocal microscopy

In confocal microscopy, out-of-focus image information is selectively discarded by placing a pin hole in front of the camera (Fig. 6). This allows collection of image-slices that contain primarily in-focus image information. By scanning the sample along the focal axis, multiple such image-slices through the sample are collected, and this enables a 3D reconstruction of the sample surface. Numerous alternative

implementations and variations on this basic method of data acquisition have been published. This is one of the most widely used TF imaging methods, particularly in biology.

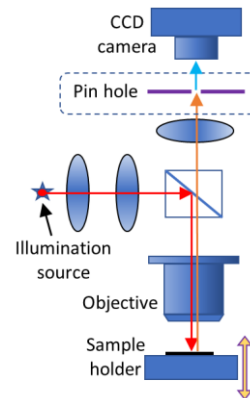


Fig. 6 Basic schematic of a confocal microscopy setup. The pin hole selectively discards out-of-focus images information.

3.12 Light sheet microscopy (LSM)

In LSM, the sample (usually transparent or semi-transparent) is illuminated from the side using a thin sheet of light. Typically, the light source is rigidly coupled to the objective and aligned with its focal plane (Fig. 7) (68-70). By scanning the sample stage along the focal axis, volumetric images of the specimen can be obtained. In a strict sense, this method is not a TF method because the imaging plane is always in focus. However, it can extract 3D volumetric image information similarly to a confocal microscope. Unlike a confocal microscope, however, the out-of-focus image information is not discarded, it is simply not illuminated. Numerous variations of this basic technique have been published (69, 71). LSM is mainly used to study biological tissues. Because of the opacity of such tissues, three-dimensional imaging is typically limited to a depth of 500 μm to 1000 μm (72, 73). However, in some studies LSM appears to outperform confocal microscopy (10).

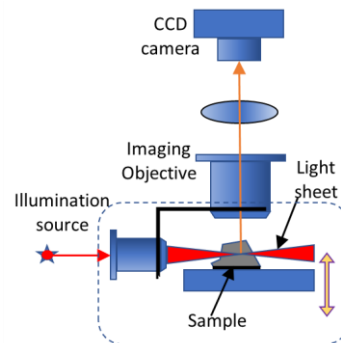


Fig. 7 Simplified schematic of LSM. In the basic setup, the imaging and illuminating objectives are rigidly coupled. The

sample is scanned along the focal axis to collect volumetric images.

3.13 Light Field Microscopy (LFM)

In this microscopy, a microlens array is inserted into the optical train of a conventional microscope between the main lens and sensor plane, and this enables the capture of light-fields of specimens in a single image (Fig. 8) (74, 75). TF images can then be extracted through application of 3D deconvolution to this single image. LFM also has the capability to extract different perspective views from the single image. In an LFM, spatial resolution is determined by the number of micro-lenses. A disadvantage of LFM is the trade-off between spatial resolution and angular resolution (74).

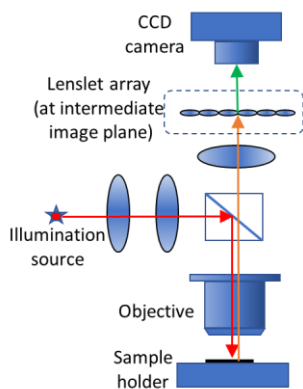


Fig. 8 Simplified schematic of LFM. The lenslet arrays are located at the intermediate image plane.

3.14 Phase retrieval techniques

Phase retrieval techniques make use of the relationship between phase and propagation direction in an optical microscope. This method initially requires a few TF images which are inverted to recover phase and amplitude quantitatively. By making use of the retrieved phase and the amplitude, the entire set of TF images can then be calculated (76-78). A variation of this method, which is sometimes called quantitative phase imaging, has found many useful applications in biology (79).

3.15 Digital holography microscopy

Holographic microscopy (including digital holography) is a coherent imaging system, and its advantage lies in the instantaneous and quantitative acquisition of both amplitude and the phase information from the reconstruction of the wave-front (80-86). Digital holography microscopy can numerically extract TF images from a single experimentally

recorded hologram without the need to move the sample (Fig. 9). The digital holographic approach has been successfully implemented to speed up TSOM image acquisition (31). Since no mechanical scanning is involved, and a complete set of TF images can be extracted from a single holographic image, it is a high-speed TF imaging method.

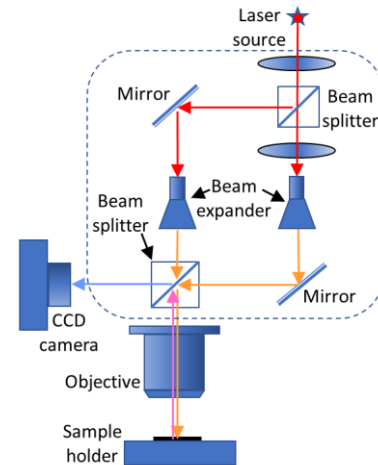


Fig. 9 Simplified schematic of DHM.

3.16 Other methods

Acousto-optic lens scanning (17) can achieve a pure focal scan at a very high speed (≈ 400 kHz). This is accomplished using two adjacent counterpropagating acoustic waves with a synchronized frequency chirp so that the transverse scans subtract to cancel each other, whereas the focal scans add. Acousto-optic modulators (AOM) and acousto-optic scanners (AOS) are used along with a laser beam, and there is a 180° phase shift between the two frequency-modulating signals. The light is focused on a CCD camera that is mounted on a translation stage and used to measure the focal distance. Temporal and spatial focusing (87) achieves high TF speeds with no moving parts. Full-field optical coherence microscopy produces volumetric imaging with all in-focus images similar to confocal microscopy (88, 89). It is based on the spatial coherence gate principle and generates in parallel complete two-dimensional TF type images without scanning.

Many variations of the preceding general TF methods have also been published. Some are a combination of two (or more) TF methods with some other method. For example, a combination of high speed sinusoidal vibration of the microscope objective along with 'smart' movements of galvanometric x-y scanners (to repeatedly scan the laser focus along a closed 3D trajectory) enables high-speed acquisition of TF images for two-photon microscopy that permits fast fluorescence measurements (14).

Optical images like the TSOM images (Fig. 1(e)) can be constructed using any one of the TF method presented here. However, for the TF methods such as confocal and light-sheet microscopy, all the images are in-focus creating a different type of TSOM image.

4 TF images categorization

4.1 Optical data type

TF optical images can be broadly divided into three types depending on the type of optical data

I. In the first type, the set of TF images usually contains a best focus image, along with many out-of-focus (or blurred) images on the either sides of the best focus image. A typical example for this type of TF data collection is the conventional stage-scanning method (37).

II. In the second type, nearly all the TF images are either in-focus or contain only in-focus image information enabling one to visualize or reconstruct the 3D volume of the sample. Confocal microscopy (42, 90) is a typical example for this kind of TF data collection method. Some TF methods are able to extract both the first and the second types of TF optical data such as the digital holography (82) method.

III. The third type, which is often referred to as either super-resolution microscopy (4) or nanoscopy (1), is a highly localized imaging method with measurement resolution down to tens of nanometers. In this stochastic approach only a small subset of molecules is switched on in a given 3D volume at any particular moment in time using fluorescence principle while the majority remains in a non-fluorescent “dark” or “off” state (91). Super-resolved images are reconstructed from the positions of thousands to millions of single molecules that have been recorded in thousands of camera frames (92). Several thorough review articles have been published on this subject (1-5), and hence no further discussion of this type of TF imaging is included in this review.

4.2 Scanning

Depending on the presence or absence of scanning, TF image collection methods can be divided into two groups.

I. In the first group, the TF image collection involves scanning (or continuous variation) of some parts of optical microscope. Typical examples include objective scanning, and light-sheet microscopy. Even though the phase retrieval technique does not require scanning, it still requires at least two images at different focal planes.

II. In the second group of methods, no scanning is involved to acquire TF images. Multi-focus microscopy and

digital holography microscopy are typical examples of this group.

4.3 Image extraction

Depending on the image extraction method two groups of TF approaches can be formed

I. Some TF methods enable direct image acquisition, such as stage scanning, liquid-tunable lens etc.

II. Some TF methods require indirect extraction (or computational extraction) of TF images. Phase retrieval and digital holographic microscopy are typical examples for this group.

A complete categorization of all the TF methods is presented in Table 1.

5 Speed and quality of TF image collection

One of the main challenges in modern optical microscopy is fast and sensitive acquisition of TF data (11, 38). In some applications such as in single molecule tracking methods (38, 41), it is essential to have a high-speed TF image collection. In contrast, for certain reference metrology applications high-speed collection may not be necessary, but high precision is of paramount necessity (24, 25). In the following sections, we discuss relative speeds and quality of TF image collection methods.

5.1 Speed

The speed of TF image collection and image quality will usually trend in opposite directions. In this review, the image quality mostly refers to signal-to-noise ratio. Typically, higher collection speeds reduce image quality, and vice versa. In the scanning-based image collection methods, TF image collection time can vary considerably depending on the microscope conditions such as exposure time, the number of TF images needed, illumination source intensity, sample type, and method of scanning. All such factors must be optimized to achieve a suitable, low-noise image in the acceptable condition. Increasing the exposure time and the number of TF images will usually increase collection time, while increasing illumination source intensity decreases it due to lesser required exposure time. A sample that returns a large scattered intensity is beneficial in reducing the exposure time and hence TF image collection time. TF collection times of the scanning methods span from a relatively slow (in the order of minutes) to a relatively high-speed (in the order of less than a ms).

Section No.	TF method	TF image data includes	Scanning	Scanning method	Image extraction	Best speeds [#]
3.1	Stage scanning	In-focus & out-of-focus	Yes	Stage	Direct	A few hundreds of ms
3.2	Objective scanning	In-focus & out-of-focus	Yes	Objective	Direct	A few hundreds of ms
3.3	Image plane scanning	In-focus & out-of-focus	Yes	Camera	Direct	A few hundreds of ms
3.4	Multifocal plane microscopy	In-focus & out-of-focus	No	NA	Direct	High-speed / Instantaneous ^{***}
3.5	Wavelength scanning	In-focus & out-of-focus	Yes	Wavelength	Direct	A few hundreds of ms
3.6	Flexible-membrane liquid lens	In-focus & out-of-focus	Yes	Focus	Direct	A few ms
3.7	Liquid-tunable lens	In-focus & out-of-focus	Yes	Focus	Direct	A few ms
3.8	Adaptive optics	In-focus & out-of-focus	Yes	Focus	Direct	A few ms
3.9	Multi-focus microscopy	In-focus & out-of-focus	No	NA	Direct	High-speed / Instantaneous ^{***}
3.10	Aperture-scanning Fourier ptychography	In-focus & out-of-focus	Yes*	NA	Computational	Tens of seconds ^{##}
3.11	Confocal microscopy	In-focus only	Yes	Stage	Direct	A few hundreds of ms
3.12	Light sheet microscopy	In-focus only	Yes	Stage	Direct	A few hundreds of ms
3.13	Light Field Microscopy	In-focus & out-of-focus	No	NA	Computational	High-speed / Instantaneous ^{***,##}
3.14	Phase retrieval techniques	In-focus & out-of-focus	Yes/No ^{**}	Any ^{**}	Computational	High-speed / Instantaneous ^{***,##}
3.15	Digital holography microscopy	In-focus & out-of-focus	No	NA	Computational	High-speed / Instantaneous ^{***,##}

*Scanning of an aperture

**Either scanning or non-scanning methods can be used to obtain a few images at different focal positions

*** Either only one image or several images simultaneously are collected

NA - Not applicable

Approximate values to collect a set of TF images

plus computational time

Table 1. A tabulation of complete categorization of the TF scanning methods.

Scanning can either be performed continuously or by using repeated, short, step-scans for the scanning-based TF image collection methods. In continuous-scanning approaches, the scanning part and the camera are synchronized which enables relatively high-speed TF image collections. For example, in the objective scanning method (section 3.2), it is possible to continuously scan the objective back-and-forth and simultaneously record images at a relatively high-speed (200 ms (41)). The focus step size depends on the time gap

between each exposure and the scanning speed of the objective. Even though the adaptive optics method (section 3.8) is a type of continuous-scanning method, it achieves a very high-speed collection (≈ 1 kHz (32)). Acousto-optic lens (≈ 400 kHz) (17), liquid lenses (2 ms / 500 Hz) (11, 93) and adaptive optics (10 ms / 100 Hz) (66) can also achieve a high-speed TF image collection.

Step-scan methods are relatively slow as scanning must be stopped briefly for image collection at every step, and this increases the overall TF image collection time. For example, in the stage scanning method (section 3.1) each time the stage is axially translated at a given step size it is stopped for image collection, repeating the process until all the TF images are collected.

Usually, non-scanning methods are relatively fast. For example, in multi-focus microscopy, TF images are collected simultaneously in one exposure (or in one image). This results in TF image collection as fast as any single image collection using a conventional microscope. Multifocal plane microscopy also can collect TF images simultaneously at a high-speed. However, the number of images is restricted to the number of times imaging beam is split. High-speed TF imaging can also be achieved using DHM. A summary of the best speeds possible to collect a set of TF images for different TF methods is presented in Table 1.

5.2 Image quality

Not all TF imaging methods produce the same quality images. In fact, a wide range of image qualities can be expected depending on the TF method and the experimental conditions. It is the opinion of the author that the best quality images can be collected relatively easily using step-scan type of TF methods (e.g., stage scanning method), but this is at the expense of collection speed. The presence of optical tool mechanical instability and other mechanical vibrations can deteriorate the image quality. In reality, scanning based methods are usually prone to image deterioration of this kind (34). Consequently, if careful attention is not given to these factors, the continuous-scanning methods will usually result in lower quality images. Liquid-tunable lenses and flexible membrane liquid lenses suffer from significant aberrations (56) which reduce image quality. Image quality in multi-focus microscopy can suffer because of splitting of the primary beam into several images.

As presented above, every TF method has certain advantages and disadvantages. The selection of a TF method depends on several factors, including type of data needed, image quality, applicability, speed of acquisition, cost, mechanical stability, accuracy, noise, simplicity, ease of use and availability of the technology. Several aspects of optical microscopes have been identified to minimize degradation of optical images (e.g., laser stability, flat-field correction, camera performance, optical aberrations, noise, spectral reproducibility, lateral resolution, lens cleanliness, lens characteristics, temporal variability of signal and noise, absolute intensity calibration, correcting field-dependent aberrations (90, 94-102)). However, to the best of our knowledge there is no published method to test the fidelity of

a set of TF images. Two aspects are uniquely associated with TF type of data collection: (i) focus step size, and (ii) sample/stage vibration (or lateral movement) during mechanical scanning. Either imprecise focus step size (including in the extracted TF images) or lateral displacement of sample is highly likely to deteriorate TF optical data. A combination of (i) and (ii) could also be present. For example, scanning methods could have mechanical instabilities and vibration issues (34) resulting in increased overall noise. If there is a mismatch between the sample stage scan axis with the optical axis along the focus direction, TF optical images appear to shift laterally (32) creating a large error. Similar lateral image shift can also be observed if the aperture diaphragm is not correctly aligned with the optical axis (20). For these reasons, it is important to evaluate fidelity of the TF data. We are actively working to develop a method to test TF data fidelity.

6 Conclusion

We have presented a review of over 15 distinct TF imaging methods from the literature. There is a wide choice to select from depending on the need. As with any optical images, the set of TF images collected using any method or under any conditions needs to be tested for fidelity. We hope to present such a test in the near future.

Disclosure

The author declares no conflict of interest

References

1. S. W. Hell, "Far-Field Optical Nanoscopy," in *Single Molecule Spectroscopy in Chemistry, Physics and Biology: Nobel Symposium A*. Gräslund, R. Rigler, and J. Widengren, Eds., pp. 365-398, Springer Berlin Heidelberg, Berlin, Heidelberg (2010).
2. R. Zenobi, "Analytical tools for the nano world," *Anal Bioanal Chem* **390**(1), 215-221 (2008).
3. S. Doose, "Trends in Biological Optical Microscopy," *ChemPhysChem* **9**(4), 523-528 (2008).
4. L. Schermelleh, R. Heintzmann, and H. Leonhardt, "A guide to super-resolution fluorescence microscopy," *The Journal of Cell Biology* **190**(2), 165-175 (2010).
5. W. H. Stefan et al., "The 2015 super-resolution microscopy roadmap," *Journal of Physics D: Applied Physics* **48**(44), 443001 (2015).
6. M. J. Rust, M. Bates, and X. Zhuang, "Sub-diffraction-limit imaging by stochastic optical reconstruction microscopy (STORM)," *Nat Methods* **3**(793) (2006).

7. E. Betzig et al., "Imaging Intracellular Fluorescent Proteins at Nanometer Resolution," *Science* **313**(5793), 1642-1645 (2006).
8. K. Fujita, "Follow-up review: recent progress in the development of super-resolution optical microscopy," *Microscopy* **65**(4), 275-281 (2016).
9. A. von Diezmann, Y. Shechtman, and W. E. Moerner, "Three-Dimensional Localization of Single Molecules for Super-Resolution Imaging and Single-Particle Tracking," *Chem Rev* **117**(11), 7244-7275 (2017).
10. A. Azaripour et al., "Three-dimensional histochemistry and imaging of human gingiva," *Sci Rep-Uk* **8**(1), 1647 (2018).
11. G. Katona et al., "Fast two-photon in vivo imaging with three-dimensional random-access scanning in large tissue volumes," *Nat Methods* **9**(201) (2012).
12. P. Prabhat et al., "Simultaneous imaging of different focal planes in fluorescence microscopy for the study of cellular dynamics in three dimensions," *IEEE Transactions on NanoBioscience* **3**(4), 237-242 (2004).
13. A. Tahmasbi et al., "Designing the focal plane spacing for multifocal plane microscopy," *Opt Express* **22**(14), 16706-16721 (2014).
14. W. Göbel, B. M. Kampa, and F. Helmchen, "Imaging cellular network dynamics in three dimensions using fast 3D laser scanning," *Nat Methods* **4**(73) (2006).
15. K. F. Tehrani et al., "Fast axial scanning for 2-photon microscopy using liquid lens technology," *SPIE BiOS* **6** (2017).
16. N. Ji, J. Freeman, and S. L. Smith, "Technologies for imaging neural activity in large volumes," *Nat Neurosci* **19**(1154) (2016).
17. A. Kaplan, N. Friedman, and N. Davidson, "Acousto-optic lens with very fast focus scanning," *Opt Lett* **26**(14), 1078-1080 (2001).
18. R. Attota et al., "Nanoparticle size determination using optical microscopes," *Appl Phys Lett* **105**(16), (2014).
19. H. Kang et al., "A method to determine the number of nanoparticles in a cluster using conventional optical microscopes," *Appl Phys Lett* **107**(10), (2015).
20. R. K. Attota, and H. Park, "Optical microscope illumination analysis using through-focus scanning optical microscopy," *Opt Lett* **42**(12), 2306-2309 (2017).
21. R. K. Attota et al., "Feasibility study on 3-D shape analysis of high-aspect-ratio features using through-focus scanning optical microscopy," *Opt Express* **24**(15), 16574-16585 (2016).
22. R. K. Attota, and H. Kang, "Parameter optimization for through-focus scanning optical microscopy," *Opt Express* **24**(13), 14915-14924 (2016).
23. R. Attota, "Noise analysis for through-focus scanning optical microscopy," *Opt Lett* **41**(4), 745-748 (2016).
24. R. Attota, and R. G. Dixon, "Resolving three-dimensional shape of sub-50 nm wide lines with nanometer-scale sensitivity using conventional optical microscopes," *Appl Phys Lett* **105**(4), (2014).
25. R. Attota, B. Bunday, and V. Vartanian, "Critical dimension metrology by through-focus scanning optical microscopy beyond the 22 nm node," *Appl Phys Lett* **102**(22), (2013).
26. A. Arceo, B. Bunday, and R. Attota, "Use of TSOM for sub-11 nm node pattern defect detection and HAR features," *Metrology, Inspection, and Process Control for Microlithography Xxvii* **8681**((2013).
27. A. Arceo et al., "Patterned Defect & CD Metrology by TSOM Beyond the 22 nm Node," *Proc Spie* **8324**((2012).
28. R. Attota, and R. Silver, "Nanometrology using a through-focus scanning optical microscopy method," *Meas Sci Technol* **22**(2), (2011).
29. R. Attota et al., "TSOM Method for Semiconductor Metrology," *Proc. SPIE* **7971**(79710T) (2011).
30. R. Attota, T. A. Germer, and R. M. Silver, "Through-focus scanning-optical-microscope imaging method for nanoscale dimensional analysis," *Opt Lett* **33**(17), 1990-1992 (2008).
31. S.-W. Park, J. H. Lee, and H. Kim, "3D digital holographic semiconductor metrology using Fourier Modal Method," in *JSAP-OSA Joint Symposia*, p. 8a_PB2_1, OSA, Fukuoka, Japan (2017).
32. S. Han et al., "Tip/tilt-compensated through-focus scanning optical microscopy," *Proc. of SPIE* **10023**(100230P) (2016).
33. M. Ryabko et al., "Through-focus scanning optical microscopy (TSOM) considering optical aberrations: practical implementation," *Opt Express* **23**(25), 32215-32221 (2015).
34. M. Ryabko et al., "Motion-free all optical inspection system for nanoscale topology control," *Opt Express* **22**(12), 14958-14963 (2014).
35. S. N. KOPTYAEV, RYABKO, M.V., HCHERBAKOV, A.V., LANTSOV, A.D., "Optical measuring system and method of measuring critical size " USPTO, Ed., USA (2014).
36. S. Usha, Shashikumar, P.V., Mohankumar, G.C., Rao, S.S., "Through Focus Optical Imaging Technique To Analyze Variations In Nano-Scale Indents," *International Journal of Engineering Research & Technology* **2**(5), 18 (2013).
37. M. V. Ryabko et al., "Method for optical inspection of nanoscale objects based upon analysis of their defocused images and features of its practical implementation," *Opt Express* **21**(21), 24483-24489 (2013).
38. S. Abrahamsson et al., "Fast multicolor 3D imaging using aberration-corrected multifocus microscopy," *Nat Methods* **10**(1), 60-U80 (2013).
39. S. Abrahamsson et al., "Multifocus microscopy with precise color multi-phase diffractive optics applied in functional neuronal imaging," *Biomed Opt Express* **7**(3), 855-869 (2016).

40. S. Abrahamsson et al., "MultiFocus Polarization Microscope (MF-PolScope) for 3D polarization imaging of up to 25 focal planes simultaneously," *Opt Express* **23**(6), 7734-7754 (2015).
41. J. M. Gineste et al., "Three-dimensional automated nanoparticle tracking using Mie scattering in an optical microscope," *Journal of microscopy* **243**(2), 172-178 (2011).
42. M. Minsky, "Memoir on Inventing the Confocal Scanning Microscope," *Scanning* **10**(4), 128-138 (1988).
43. W. E. Ortyn et al., "Extended depth of field imaging for high speed cell analysis," *Cytom Part A* **71A**(4), 215-231 (2007).
44. R. Attota et al., "Optical critical dimension measurement and illumination analysis using the through-focus focus metric - art. no. 61520K," *P Soc Photo-Opt Ins* **6152**(K1520-K1520 (2006).
45. R. Attota et al., "Application of through-focus focus-metric analysis in high resolution optical metrology," *Metrology, Inspection, and Process Control for Microlithography XIX, Pts 1-3* **5752**(1441-1449 (2005).
46. R. M. Silver et al., "High-resolution optical overlay metrology," *Metrology, Inspection, and Process Control for Microlithography Xviii, Pts 1 and 2* **5375**(78-95 (2004).
47. R. M. Silver et al., "Scatterfield microscopy for extending the limits of image-based optical metrology," *Appl Optics* **46**(20), 4248-4257 (2007).
48. B. M. Barnes et al., "Optical volumetric inspection of sub-20nm patterned defects with wafer noise," *SPIE Advanced Lithography* **10** (2014).
49. R. K. Attota, "Step beyond Kohler illumination analysis for far-field quantitative imaging: angular illumination asymmetry (ANILAS) maps," *Opt Express* **24**(20), 22616-22627 (2016).
50. R. Attota, and R. Silver, "Optical microscope angular illumination analysis," *Opt Express* **20**(6), 6693-6702 (2012).
51. E. A. Patterson, and M. P. Whelan, "Optical Signatures of Small Nanoparticles in a Conventional Microscope," *Small* **4**(10), 1703-1706 (2008).
52. E. J. Botcherby et al., "An optical technique for remote focusing in microscopy," *Opt Commun* **281**(4), 880-887 (2008).
53. A. Jesacher, C. Roider, and M. Ritsch-Marte, "Enhancing diffractive multi-plane microscopy using colored illumination," *Opt Express* **21**(9), 11150-11161 (2013).
54. G. C. Knollman, J. L. S. Bellin, and J. L. Weaver, "Variable-Focus Liquid-Filled Hydroacoustic Lens," *J Acoust Soc Am* **49**(1), 253-& (1971).
55. C. Friese et al., "Materials, effects and components for tunable micro-optics," *Ieej T Electr Electr* **2**(3), 232-248 (2007).
56. P. P. Zhao, C. Ataman, and H. Zappe, "Miniaturized variable-focus objective employing a liquid-filled tunable aspherical lens," *Opt Eng* **56**(10), (2017).
57. L. H. Wang, H. Oku, and M. Ishikawa, "Paraxial ray solution for liquid-filled variable focus lenses," *Jpn J Appl Phys* **56**(12), (2017).
58. L. Wang et al., "Variable-Focus Liquid Lens Integrated with a Planar Electromagnetic Actuator," *Micromachines-Basel* **7**(10), (2016).
59. W. X. Zhao et al., "Variable-focus cylindrical liquid lens array," *International Conference on Optics in Precision Engineering and Nanotechnology (Icopen2013)* **8769**((2013).
60. P. Pokorný et al., "Deformation of a prestressed liquid lens membrane," *Appl Optics* **56**(34), 9368-9376 (2017).
61. H. Ren, and S.-T. Wu, "Variable-focus liquid lens," *Opt Express* **15**(10), 5931-5936 (2007).
62. J.-W. Du, X.-Y. Wang, and D. Liang, "Bionic optical imaging system with aspheric solid-liquid mixed variable-focus lens," **11** (2016).
63. H. Ren, and S. T. Wu, "Variable-focus liquid lens by changing aperture," *Appl Phys Lett* **86**(21), (2005).
64. D. Koyama, R. Isago, and K. Nakamura, "Compact, high-speed variable-focus liquid lens using acoustic radiation force," *Opt Express* **18**(24), 25158-25169 (2010).
65. P. S. Salter, Z. Iqbal, and M. J. Booth, "Analysis of the Three-Dimensional Focal Positioning Capability of Adaptive Optic Elements," *International Journal of Optomechatronics* **7**(1), 1-14 (2013).
66. M. Žurauskas et al., "Rapid adaptive remote focusing microscope for sensing of volumetric neural activity," *Biomed Opt Express* **8**(10), 4369-4379 (2017).
67. S. Dong et al., "Aperture-scanning Fourier ptychography for 3D refocusing and super-resolution macroscopic imaging," *Opt Express* **22**(11), 13586-13599 (2014).
68. T. F. Holekamp, D. Turaga, and T. E. Holy, "Fast Three-Dimensional Fluorescence Imaging of Activity in Neural Populations by Objective-Coupled Planar Illumination Microscopy," *Neuron* **57**(5), 661-672 (2008).
69. R. M. Power, and J. Huisken, "A guide to light-sheet fluorescence microscopy for multiscale imaging," *Nat Methods* **14**(360 (2017).
70. J. Huisken et al., "Optical Sectioning Deep Inside Live Embryos by Selective Plane Illumination Microscopy," *Science* **305**(5686), 1007-1009 (2004).
71. A.-K. Gustavsson et al., "3D single-molecule super-resolution microscopy with a tilted light sheet," *Nature Communications* **9**(1), 123 (2018).
72. B. Weigelin, G.-J. Bakker, and P. Friedl, "Third harmonic generation microscopy of cells and tissue organization," *Journal of Cell Science* **129**(2), 245-255 (2016).
73. T. Lagerweij et al., "Optical clearing and fluorescence deep-tissue imaging for 3D quantitative analysis of the

- brain tumor microenvironment," *Angiogenesis* **20**(4), 533-546 (2017).
74. M. Zhang et al., "Three-dimensional light field microscope based on a lenslet array," *Opt Commun* **403**(Supplement C), 133-142 (2017).
 75. M. Levoy et al., "Light field microscopy," *ACM Trans. Graph.* **25**(3), 924-934 (2006).
 76. L. J. Allen, and M. P. Oxley, "Phase retrieval from series of images obtained by defocus variation," *Opt Commun* **199**(1), 65-75 (2001).
 77. Z. Jingshan et al., "Transport of Intensity phase imaging by intensity spectrum fitting of exponentially spaced defocus planes," *Opt Express* **22**(9), 10661-10674 (2014).
 78. B. Xue et al., "Transport of intensity phase imaging from multiple intensities measured in unequally-spaced planes," *Opt Express* **19**(21), 20244-20250 (2011).
 79. G. Popescu, *Quantitative phase imaging of cells and tissues*, McGraw-Hill, New York (2011).
 80. S. S. Kou, and C. J. R. Sheppard, "Imaging in digital holographic microscopy," *Opt Express* **15**(21), 13640-13648 (2007).
 81. M. Matrecano, M. Paturzo, and P. Ferraro, "Extended focus imaging in digital holographic microscopy: a review," **19** (2014).
 82. T. Colomb et al., "Extended depth-of-focus by digital holographic microscopy," *Opt Lett* **35**(11), 1840-1842 (2010).
 83. J. P. Ryle et al., "Calibration of a digital in-line holographic microscopy system: depth of focus and bioprocess analysis," *Appl Optics* **52**(7), C78-C87 (2013).
 84. P. Ferraro et al., "Extended focused image in microscopy by digital holography," *Opt Express* **13**(18), 6738-6749 (2005).
 85. J. Rosen, and G. Brooker, "Fresnel incoherent correlation holography (FINCH): a review of research," in *Advanced Optical Technologies*, p. 151 (2012).
 86. P. Ferraro et al., "Compensation of the inherent wave front curvature in digital holographic coherent microscopy for quantitative phase-contrast imaging," *Appl Optics* **42**(11), 1938-1946 (2003).
 87. M. E. Durst, G. Zhu, and C. Xu, "Simultaneous spatial and temporal focusing for axial scanning," *Opt Express* **14**(25), 12243-12254 (2006).
 88. A. Dubois et al., "High-resolution full-field optical coherence tomography with a Linnik microscope," *Appl Optics* **41**(4), 805-812 (2002).
 89. E. Beaufort et al., "Full-field optical coherence microscopy," *Opt Lett* **23**(4), 244-246 (1998).
 90. R. M. Zucker, and O. Price, "Evaluation of confocal microscopy system performance," *Cytometry* **44**(4), 273-294 (2001).
 91. T. J. Gould, S. T. Hess, and J. Bewersdorf, "Optical Nanoscopy: From Acquisition to Analysis," *Annual Review of Biomedical Engineering* **14**(1), 231-254 (2012).
 92. F. Huang et al., "Ultra-High Resolution 3D Imaging of Whole Cells," *Cell* **166**(4), 1028-1040 (2016).
 93. H. Oku, and M. Ishikawa, "Rapid liquid variable-focus lens with 2-ms response," *Ieee Leos Ann Mtg* 947-+ (2006).
 94. R. Attota et al., "A new method to enhance overlay tool performance," *Metrology, Inspection, and Process Control for Microlithography Xvii, Pts 1 and 2* **5038**(428-436 (2003).
 95. R. M. Zucker, "Quality assessment of confocal microscopy slide-based systems: Instability," *Cytom Part A* **69A**(7), 677-690 (2006).
 96. K. M. Kedziora et al., "Method of calibration of a fluorescence microscope for quantitative studies," *Journal of microscopy* **244**(1), 101-111 (2011).
 97. J. C. Waters, and T. Wittmann, *Quantitative Imaging in Cell Biology*, First ed., Elsevier (2014).
 98. M. Halter et al., "An Automated Protocol for Performance Benchmarking a Widefield Fluorescence Microscope," *Cytom Part A* **85a**(11), 978-985 (2014).
 99. K. I. Mortensen, and H. Flyvbjerg, "Calibration-on-the-spot": How to calibrate an EMCCD camera from its images," *Sci Rep-Uk* **6**(2016).
 100. A. von Diezmann et al., "Correcting field-dependent aberrations with nanoscale accuracy in three-dimensional single-molecule localization microscopy," *Optica* **2**(11), 985-993 (2015).
 101. K. M. Douglass et al., "Super-resolution imaging of multiple cells by optimized flat-field epi-illumination," *Nat Photonics* **10**(11), 705-+ (2016).
 102. F. Huang et al., "Video-rate nanoscopy using sCMOS camera-specific single-molecule localization algorithms," *Nat Methods* **10**(7), 653-+ (2013).